

Notes on the Design of the SPAARO UAV

Justin F. Murtha*, and Craig A. Woolsey†

Virginia Polytechnic Institute and State University, Blacksburg, Virginia, 24061

These notes briefly describe the design and construction of the SPAARO (“Small Platform for Autonomous Aerial Research Operations”) UAV at Virginia Tech. The notes also include results of preliminary dynamic modeling that have been used to develop a simulation for pilot training. Details of numerical and experimental design analysis are available from the authors.

I. Aircraft Design Requirements

At the onset of design, the aircraft configuration was chosen to meet the following robustness and safety requirements. These requirements were established in order to ensure a reliable, and easily operated system and one which makes efficient use of setup time and human resources.

1. **Portable.** The UAV must be transportable, fitting easily into the Nonlinear System Laboratory’s 12 ft. trailer. To allow room for the ground control system (GCS), tools, and other assorted components, the UAV must break down into manageable subassemblies.
2. **Autonomous Capable.** The UAV must be capable of fully autonomous flight throughout the full flight envelope to enable precise and repeatable flight patterns, including auto-takeoff and auto-landing.
3. **Short, Unimproved Field Operations.** Takeoff and landing rolls must be less than 250 feet. The grass field which will serve as the primary base of operations measures 100ft X 400ft.
4. **Airdata Boom Capable.** Each aircraft must accept a Space Age Control “air data boom” for high fidelity flight data measurements. These measurements are to be used to validate modeling predictions and fine-tune the aircraft dynamic model.
5. **Easy to Assemble.** Assembly of each aircraft should take no more than 15 minutes, with an additional 15 minutes for GCS assembly. Excessive setup and breakdown procedures amplify the chance of incorrect assembly, reducing reliability.
6. **AMA Compliant Airframe.** The airframe must be built to abide by the current radio control (R/C) limits set forth by the Academy of Model Aeronautics (AMA).
7. **Segregated Payload Bays.** Two physically separated payload bays must be large enough to accommodate all necessary non flight-critical and flight-necessary payloads, respectively. Physical separation reduces the chance of disturbing or disconnecting a flight-critical component when working with mission-related components.
8. **Durable and Reliable.** Each airframe must be durable, capable of completing 100 flights per year and no fewer than 200 flight-hours per year without requiring repair or replacement of a major component (e.g., the fuselage box or main wing).
9. **Easy to Manufacture.** Each aircraft should be capable of being assembled from prefabricated or purchased parts in 60 man-hours. A total of 80 man-hours is dedicated to part fabrication and aircraft assembly, to minimize human resource requirements.

*Graduate Student, Department of Aerospace and Ocean Engineering, Member AIAA.

†Associate Professor, Department of Aerospace and Ocean Engineering, Associate Fellow AIAA.

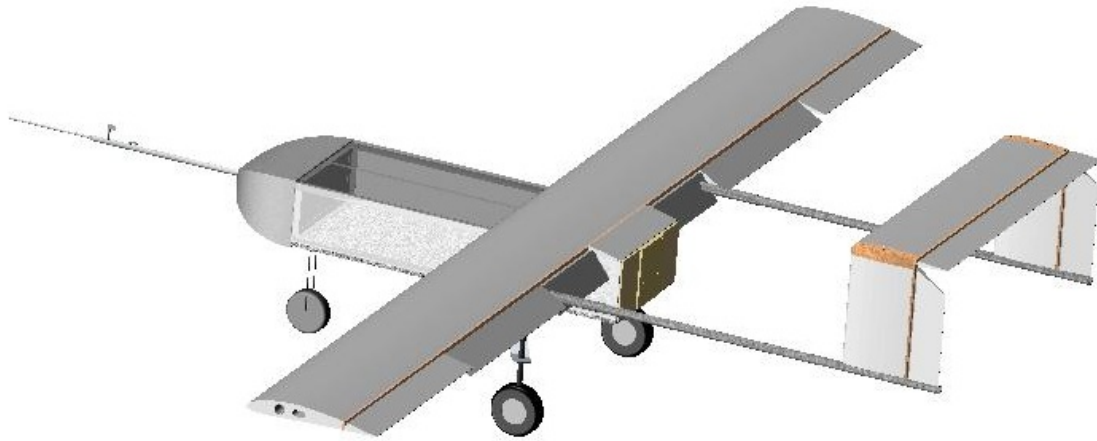


Figure 1: SPAARO UAV.

A. Reliability and Ease of Use

Pending authorization, the UAV will be used in aerobiological sampling research activities at the Kentland Farm agricultural research site. Success of this research is dependent on a reliable platform. The UAV must be capable of being prepared for flight on one day's notice. The unpredictable conditions of a grass field and relatively high wind fractions at the flight range pose an additional challenge to design. The "hands off" nature of autonomous flight requires that the control system and the aircraft structure be robust enough to consistently land safely in the flight range. Preliminary reliability studies were performed on various aspects of the aircraft using Fault Tree Analysis.¹ Control surface redundancy, component quality, cost, and basic component configurations were analyzed to help determine where reliability could easily be improved.

B. Uniformity of Aircraft

Aircraft replicants must be as identical as possible to sibling aircraft, even those fabricated after the current research program is complete. Future builders must have access to documentation detailing repeatable construction and assembly techniques.

C. Maintainability

Maintainability is a critical requirement for consistently reliable platform. Pre- and post-flight checks will be performed during each aircraft operational sortie to check for inconsistencies or damage. All parts must therefore be easily accessible for inspection, to check for fatigue or damage. Furthermore, parts that show wear and tear must be easily replaced to eliminate the chance of component failure during aircraft operation.

D. Access to Payload Bay & Fuselage Design

Nonflight-critical payloads will be physically separated from flight-critical components as a measure of safety against unintentional jostling of flight-critical components. The aim is to prevent disconnects, static discharges, and other incidental damage to flight-critical hardware. Non-flight-critical "mission" payloads will be mounted to a removable "tray" that allows bench testing of all payloads outside of the aircraft structure. When a mission payload is ready, the tray will be latched into the fuselage for flight. The fuselage design was driven by the requirement that payload bays should be accessible, spacious and modular. The design process began with estimation of the required size and geometry of expected payload components. The expected payloads were modeled in Unigraphics NX 5.0 and arranged within a box structure to obtain minimum fuselage dimensions. Figure 2 shows the initial fuselage model. Prospective payload components of known geometry were placed by trial and error to minimize the cross section. The fuel tanks were then positioned

near the expected center of gravity and wing location. Once minimum fuselage dimensions were determined and frozen, the landing gear system was designed.

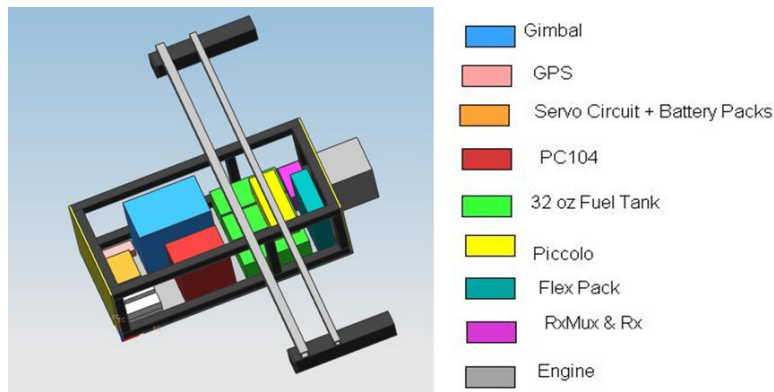


Figure 2: CAD Model of Fuselage Containing Various Payloads

II. Aircraft Design

A. Methods Used

Structural and aerodynamic testing was woven into the early stages of design to learn what construction methods were feasible before design choices were frozen. For configuration design and initial sizing, designers referred to the commonly used aircraft design textbook by Raymer.² Preliminary sizing techniques were taken from Roskam³ and from Jenkinson and Marchman.⁴ Structural design calculations were based on methods found in Magsom.⁵ Etkin and Reid's text⁶ was a primary reference for static and dynamic stability analysis.

The design process was modified from the traditional industry standard process (SRR, PDR, CDR, FSRB) to one that allowed for hands-on learning. The design process consisted of the following phases:

1. Configuration design and layout
2. Preliminary sizing
3. Performance and aerodynamic modeling
4. Stability and control analysis
5. Construction (with an emphasis on composite fabrication)

B. Justification of Design

The designers selected a pusher configuration with twin tailbooms and an inverted U-tail. This configuration accommodates the robustness requirements in Section I and allows for a modular payload bay in the front, separating the flight-critical from non-flight-critical payloads. One can simply “open the hood” of the payload bay to access the mission payload. The SPAARO will use flaps for a shortened takeoff roll and to achieve slower landing speeds. The main wing divides into three sections - a center section acting as the structural joint for the tailbooms and two outer wing sections. Each outer wing section has an aileron and flap (of equal dimensions to simplify manufacturing). Additionally, the center wing section has a flap on either side of the fuselage. The six control surfaces on the wing provide redundant control surfaces, allowing the future implementation of a fault-tolerant flight control system. Figure 3 illustrates the planform and control surface locations.

C. Structural Design

The SPAARO structure was designed to be reliable, reproducible and easily fabricated. The small scale of the airplane allowed a twofold structural design method. A traditional structural analysis model was

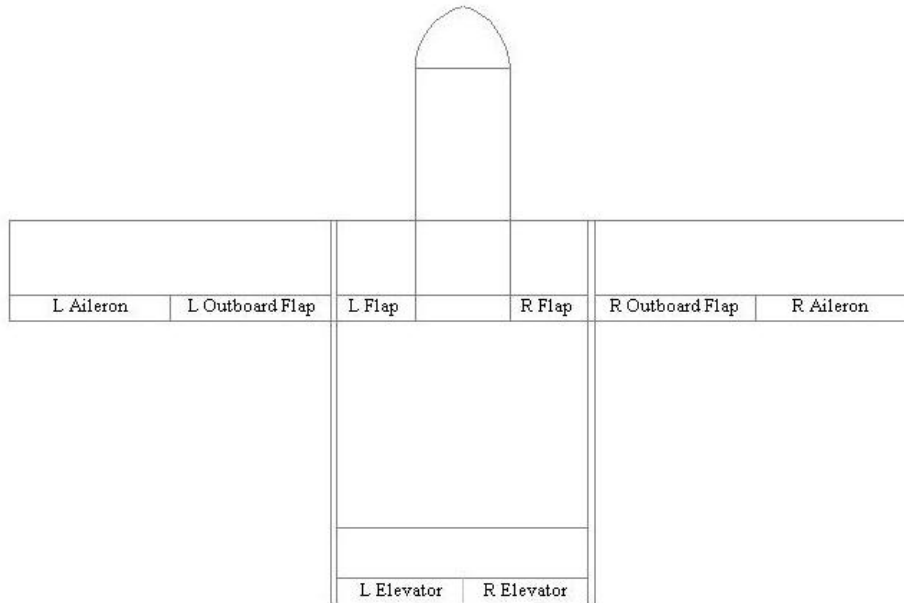


Figure 3: Sketch of overall planform & Control Surfaces

complemented by a rapid iterative process of design, build and test. The more efficient method was determined on a case-by-case basis. Analysis was performed when the structure was of a regular shape with well defined loads and boundary conditions. Wing tip deflections were calculated from various spar shapes and sizes and the final spar was sized to deflect a maximum of 4 inches at 3g's. It was discovered, however, in many instances where composites or commercially available components were used it was more efficient for the students to build and test to validate a particular design. For example, the carbon-fiber wing spar's connection was difficult to model accurately, therefore a prototype fuselage was supported by the wing spar tips and loaded to three times the expected takeoff weight. In another case, the irregularly shaped landing gear mount and struts were iteratively built and tested to withstand a worst-case scenario asymmetric 3g touchdown on one wheel.

D. Aerodynamic Design

Once the overall pusher configuration was frozen, preliminary sizing was performed to size the wing and tail surfaces. Dr. Elson Shields'^a custom built R/C research plane⁷ as seen in Figure 4 was used as the basis for initial sizing because his platform has consistently performed reliably in a similar "grass-field" environment. Initial sizing was frozen as shown in Table 1 .

| | |
|-------|-----------------------|
| MGTOW | 55 lbs |
| W/S | 55 oz/ft ² |
| Power | 5.7 hp |
| AR | 9 |

Table 1: Initial Sizing

The NACA-4412 airfoil was chosen for the main wing and NACA-0009 airfoil was chosen for tail surfaces. These were chosen because they are commonly used airfoils, and many aerodynamic tools already have co-

^aProfessor, Entomology Department, Cornell University



Figure 4: Dr. Elson Shields' Custom Built R/C Research Plane

ordinates for these airfoils. More complex shapes would require coordinate input for every tool used. One option explored was the NACA-4415 airfoil. It yields a higher lift coefficient at the expense of slightly higher form drag, however the NACA-4412 was chosen over the NACA-4415 because flaps will be used to increase lift at low speeds and the NACA-4412 offers lower drag at cruise speed.

Many COTS airframes are flown with 20% static margin. This relatively high margin, when compared to GA or other manned planes, is suggested for an ultra-stable surveillance type UAV being primarily flown by a pilot on the ground. In order to conform to this standard of practice, SPAARO will also have a 20% static margin.

Drela's Athena Vortex Lattice (AVL) code was used to generate trim conditions, Trefftz plane, 3D aerodynamic data, and stability derivatives for cruise and landing scenarios.⁸ The SPAARO model as analyzed in AVL can be seen in Figure 6. The Trefftz plane at cruise can be seen in Figure 6a. The Trefftz plane on approach can be seen in Figure 6b.

Parasitic drag was estimated from both experimental wind tunnel testing and analytical methods. Figure 7 presents a photo of wind tunnel tests being performed to find parasitic drag of the fuselage, landing gear, and engine. The tests measured a parasitic drag coefficient of 0.051.

Parasitic drag for the wing and tail sections were calculated analytically using proven skin friction and form drag assumptions. Mason's FRICTION⁹ code was used for these surfaces. The resulting parasitic drag from lifting surfaces was 0.019. Drag will also arise from wing and fuselage interaction; so an additional 0.005 was added as a safety factor to the drag buildup to help account for this. The total parasitic drag coefficient totalled 0.075.

E. Control System

The primary flight control system will be a commercially available Piccolo II autopilot manufactured by Cloud Cap Technologies^b. The Piccolo II autopilot uses a 40MHz MPC555 Power PC running a nested sequence of PID control loops to compute the various actuator commands. These loops range from critical inner loops like bank angle control to outer, navigation loops like GPS waypoint navigation. The gain tuning procedure can be performed both on the ground with hardware-in-the-loop simulations and in actual flight testing.

The SPAARO also has an onboard control signal multiplexer board to allow a standard R/C receiver to override the autopilot's servo outputs. This added safety feature allows a pilot on the ground to completely bypass the Piccolo II system and sensors in an event of a failure.

^bUAV autopilots are highly sensitive to ITAR restriction. Virginia Tech has taken meticulous steps to ensure all Piccolo II users affiliated with VT have legal access licenses.

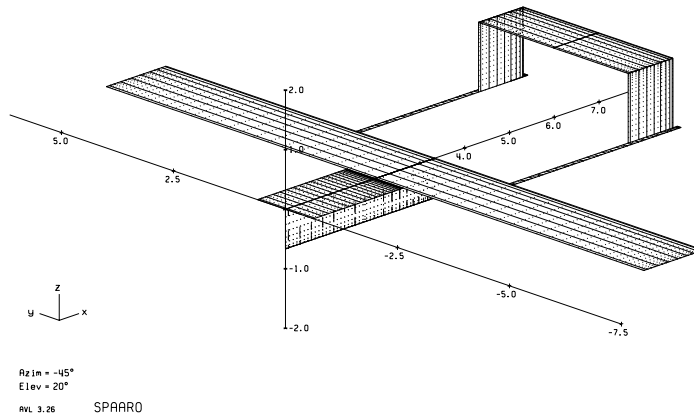
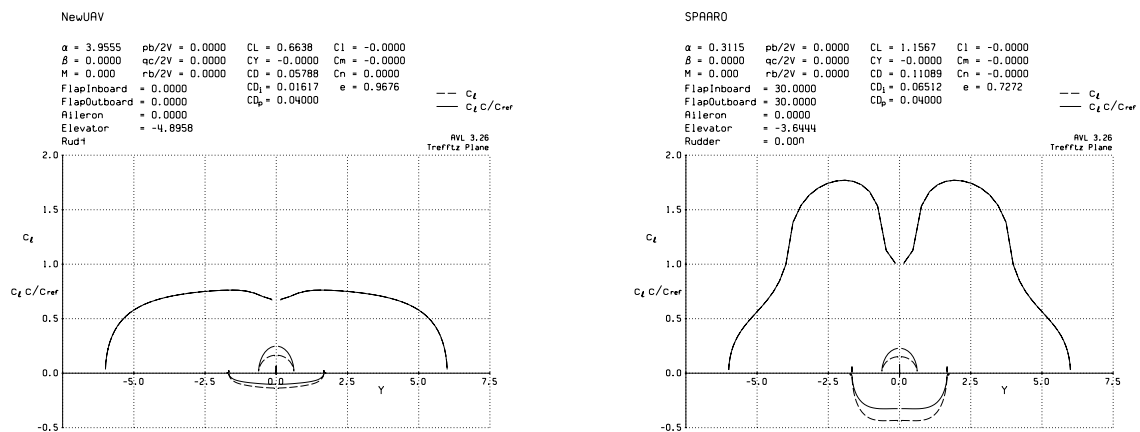


Figure 5: AVL Analysis output



(a) Trefftz Plane at Cruise

(b) Trefftz Plane on Approach

Figure 6: AVL Analysis output



Figure 7: Parasitic Drag Testing of SPAARO Fuselage in Virginia Tech Stability Wind Tunnel

F. Performance Design

Because there were few specific performance constraints given to the students, a large flight envelope was not critical to all design decisions. The envelope was calculated during design and continually updated with higher fidelity wind tunnel testing and modeling. Anderson’s aircraft performance text¹⁰ was a primary reference for performance analysis.

A key constraint was the ability to restart the engine during flight. This limited the engine selection, as only a few R/C engine manufacturers produce such an engine for this scale. The Fuji-64A with onboard starter was chosen to spin a Zinger 22X10 pusher prop. To model this propulsion system, the students used Hepperle’s JavaProp¹¹ to calculate thrust and torque at various airspeeds. JavaProp is based on propeller blade element theory, and students used the assumption of constant power. Estimates of thrust as a function of velocity can be seen in Figure 8a and estimates of propeller efficiency can be seen in Figure 8b. Scripts written with MATLAB[®] were used to generate flight envelopes for various altitudes. Key performance data is listed in Table 2.

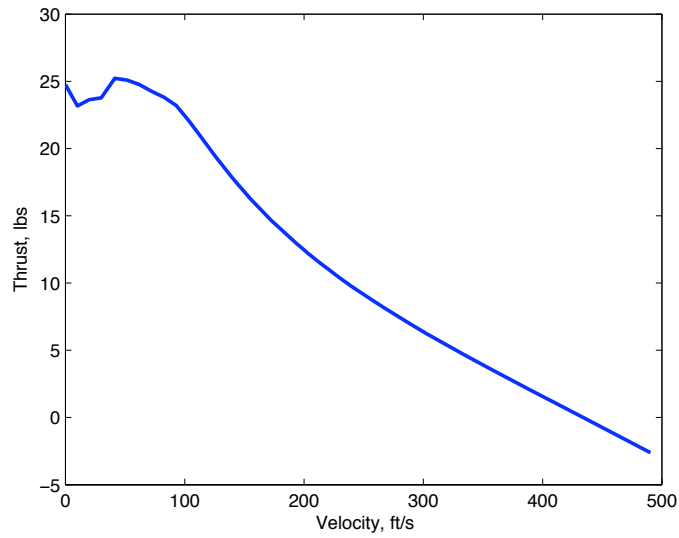
| | |
|---|----------|
| V_{\max} | 118 ft/s |
| $V_{\text{stall}}(30^\circ \text{Flaps})$ | 38 ft/s |
| $V_{h_{\max}}$ | 71 ft/s |
| h_{\max} | 1100 fpm |
| $V_{L/D_{\max}}$ | 48 ft/s |
| L/D_{\max} | 9.2 |

Table 2: Key Performance Data

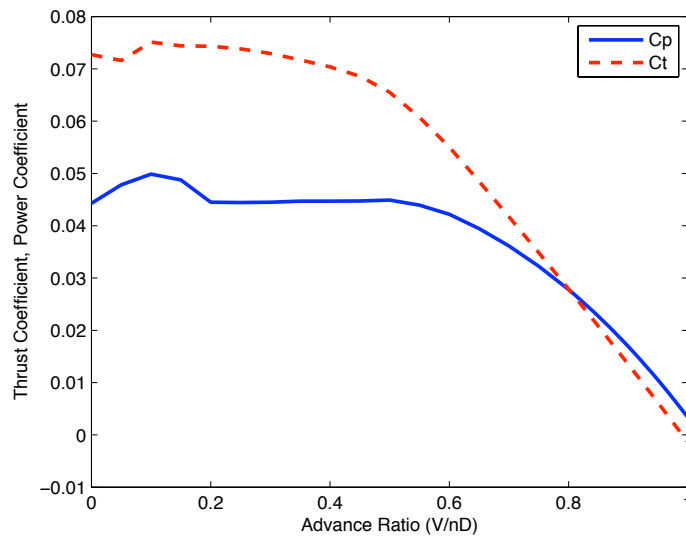
G. Air Data Instrumentation

An airdata measurement system was purchased from Space Age Control to instrument the aircraft with barometric altitude, airspeed, angle of attack, and angle of sideslip data. “The Mini Air Data Boom” (#100400) was purchased for the SPAARO to collect high-fidelity measurements, and data is recorded by the onboard PC/104 computer at 100Hz to be used in future controls logic and aircraft instrumentation. Airdata measurement system design and calibration was based on work done by Haering.¹²

The airdata boom protrudes straight out of the nose in the body axes. Because of the relatively blunt nose cone close to the sensors, asymmetric flow over the nose cone adversely affected the sensors and produced biased data. The fuselage and boom were mounted in the Virginia Tech 6 ft x 6 ft Stability Wind Tunnel



(a) Thrust - Velocity relation for propeller



(b) Propeller performance data

Figure 8: Data generated by JAVAFOIL for propeller performance estimate

to generate a calibration curve for non-zero angles of attack and sideslip. Figure 9 shows the SPAARO fuselage mounted at 22° angle of attack in Stability Tunnel.



Figure 9: SPAARO Air Data Boom Calibration in VT's Stability Wind Tunnel

H. Ground Control Station and Outer Loop Control

The SPAARO is designed to be fully autonomous, and nominally accepts only outer loop control inputs for flight. This includes GPS waypoints, velocities, and payload controls. Routine control parameters for takeoff, basic flight maneuvers, and autoland are tuned *a priori*, in hardware-in-the-loop simulation, for the nominal flight configuration and then adjusted during early flight tests.

In addition to CloudCap's Operator Interface, a LabVIEW[®] program has been created that receives all realtime autopilot telemetry data and interprets it for additional safety measures. With this software, multiple UAVs can be monitored simultaneously. A fuel consumption vs. throttle curve was generated so a realtime fuel gauge could be implemented, as proposed by Bhamidipati et al.¹³ Audible alarms were added for low battery life, low fuel, dangerously long flight time, and engine failures. Figure 10 is a screenshot of this alarm interface.

III. Aircraft Construction

The manufacturing process was strongly influenced by the requirement that current and future students be able to rapidly fabricate highly uniform airframes and airframe components. The methods chosen require minimal experience. For example, the wing and tail sections - typically tedious to construct consistently - are made with foam cores and can be quickly, and easily manufactured by simply executing a custom program on Virginia Tech's FoamLinx FCX848 Foam Cutter shown in Figure 11 .

The fabrication process has been carefully documented to assist future builders unfamiliar with the design. Components that were manufactured in-house are well documented with SolidWorks[®] CAD models, technical drawings, digital pictures, equipment manuals, material descriptions and step-by-step procedures to fabricate each part. For commercial-off-the-shelf (COTS) components, manufacturer contact information, cost and part numbers are provided. Higher-level assembly drawings to assist with the assembly of the individual parts and documentation outlining the integration of the payload, electronics, landing gear, brakes and propulsion systems are all available to the future builders for reference.

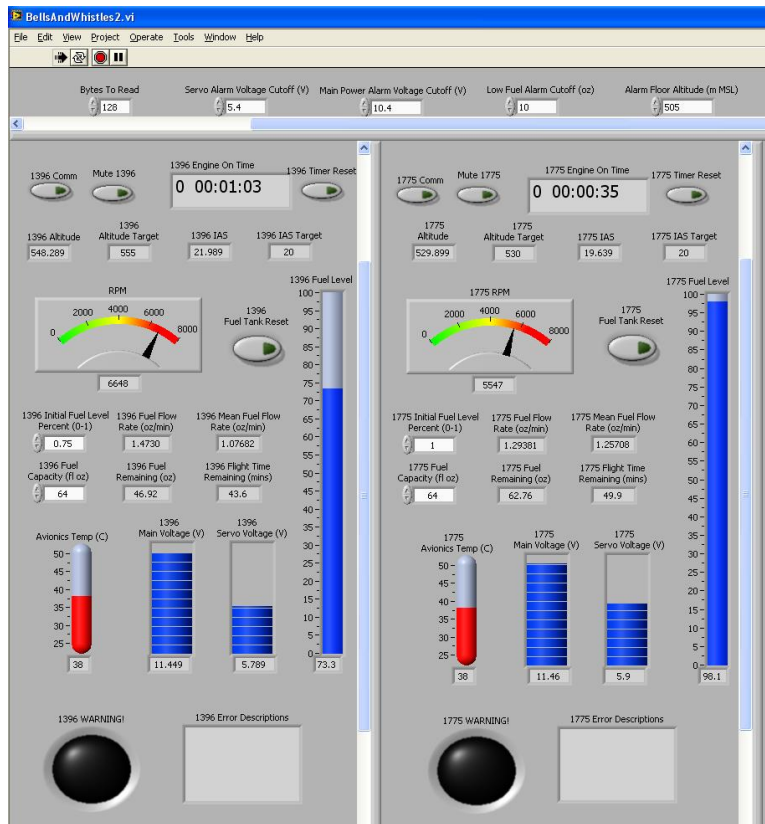


Figure 10: LabVIEW[®] Based Ground Station Alarm Interface



Figure 11: Virginia Tech's FoamLinx FCX848 Foam Cutter

IV. Aircraft Model

The SPAARO was first modeled in SolidWorks[®] 3-D CAD Software. An example of this model can be seen in Figure 13a . Using the SolidWorks[®] model as a baseline, tolerances and mechanical connections were checked to ensure that the vehicle would be properly integrated before aircraft parts were manufactured. The SolidWorks[®] model was also used as an input to AVL.⁸ AVL was used to for aerodynamic analysis of the vehicle. AVL will generate aerodynamic derivatives and plot basic 3-D forces. AVL is an extended vortex lattice code that will model arbitrary 3D lifting surfaces and fuselage bodies. It includes a full linearization of the aerodynamic model and provides trim conditions, Trefftz plane, and eigenmode analysis. Basic mass properties of the SPAARO were found using measurements and scales. The initial estimate of the moments of inertia of the SPAARO UAV were found by comparing the SPAARO to another aircraft with known mass properties. Once constructed, the bifilar pendulum method was used to more accurately determine the inertia properties. Figure 12 shows the SPAARO hung from two filaments. Predicted flight envelope data can be found in Table 3a and data describing the aircraft geometric configuration as well as mass properties can be found in Table 3b . Non-dimensional longitudinal aerodynamic derivative data that was generated with AVL can be found in Table 4 . Lateral-directional non-dimensional aerodynamic derivatives that were generated with AVL can be found in Table 5 .



Figure 12: Measuring inertia: SPAARO suspended from two filaments.

The SPAARO was also modeled using the Flightgear¹⁴ open source flight simulator. Using Flightgear, the UAV design could be tested in the context of a validated flight simulation tool. In Flightgear, users input aerodynamic coefficients, geometric data, mass data, and a 3D vehicle shape. The students created a simplified 3-D model in SolidWorks[®], and used the aerodynamic derivatives generated from AVL to define the aerodynamic characteristics. The Flightgear VMRL model can be seen in Figure 13b . A screen capture of the SPAARO flying in the Flightgear simulation can be seen in Figure 13c .

This FlightGear model will be utilized for pilot training and initial gain tuning. CloudCap provides a simulator that links the Operator Interface to FlightGear to allow pilots to fly the SPAARO under both R/C and autonomous control. Inner loop control gains will be incrementally tuned with this simulator setup to minimize flight test risk during early flight testing.

| | |
|--------------------------------|------------------|
| Max altitude | 40,000ft (MSL) |
| V_{\max} | 118 ft/sec |
| V_{NE} | 120 ft/sec |
| V_{stall} (nominal) | 46 ft/sec |
| V_{stall} (30° flaps) | 38 ft/sec |
| V_{TO} | 55 ft/sec |
| V_{Approach} | 50 ft/sec |
| Max Range from GCS | 6.2 miles (10km) |
| Takeoff distance | 165 ft |
| n_{\max} | 3 g's |

(a) Flight Envelope

| | |
|-------------------------|---------------------------|
| b | 12 ft |
| \bar{c} | 1.33 ft |
| length | 9 ft |
| x_{cg} (positive aft) | 28 inches |
| y_{cg} | 0 inches |
| z_{cg} | -4 inches |
| S | 16 ft ² |
| m | 1.71 slugs |
| I_{xx} | 4 slug ft ² |
| I_{yy} | 2 slug ft ² |
| I_{zz} | 4 slug ft ² |
| I_{xz} | -2.2 slug ft ² |

(b) Geometric and inertial properties

Table 3: Basic Aircraft Configuration Parameters

| | | | | |
|-----------|----------------|------------------------|-----------|--------------------|
| C_{D_0} | C_{D_α} | $C_{D_{\delta_e}}$ | | |
| 0.075 | .35 (est.) | 0.0033 | | |
| C_{L_0} | C_{L_α} | $C_{L_{\dot{\alpha}}}$ | C_{L_q} | $C_{L_{\delta_e}}$ |
| 0.322 | 5.31 | 0 (est.) | 9.12 | 0.526 |
| C_{m_0} | C_{m_α} | $C_{m_{\dot{\alpha}}}$ | C_{m_q} | $C_{m_{\delta_e}}$ |
| -0.049 | -1.267 | -4 (est.) | -14.52 | -1.536 |

Table 4: Longitudinal coefficients at cruise speed (65ft/s).

| | | | | |
|---------------|-----------|-----------|--------------------|--------------------|
| C_{l_β} | C_{l_r} | C_{l_p} | $C_{l_{\delta_a}}$ | $C_{l_{\delta_r}}$ |
| -0.0556 | 0.184 | -0.543 | -0.264 | -0.0118 |
| C_{n_β} | C_{n_r} | C_{n_p} | $C_{n_{\delta_a}}$ | $C_{n_{\delta_r}}$ |
| 0.0759 | -0.0697 | -0.0547 | -0.00212 | -0.0694 |
| C_{Y_β} | C_{Y_r} | C_{Y_p} | $C_{Y_{\delta_a}}$ | $C_{Y_{\delta_r}}$ |
| -0.340 | 0.188 | 0.105 | 0.0084 | 0.197 |

Table 5: Lateral-directional coefficients at cruise speed (65ft/s).

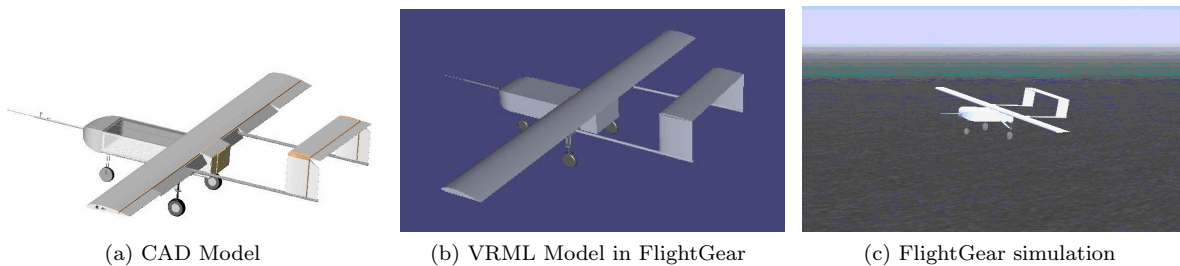


Figure 13: Various 3D Models of SPAARO

References

- ¹Roberts, N., Vesely, W., Haasl, D., and Goldberg, F., *Fault Tree Handbook*, Washington, D.C., 1981.
- ²Raymer, D. P., *Aircraft Design: A Conceptual Approach*, AIAA, Playa del Rey, California, fourth edition ed., 2000.
- ³Roskam, J., *Airplane Design Part I: Preliminary Sizing of Airplanes*, Design, Analysis and Research Corporation (DAR-corporation), University of Kansas, Lawrence, 2005.
- ⁴Jenkinson, L. R. and James F. Marchman, I., *Aircraft Design Projects*, AIAA and Butterworth-Heinemann, An imprint of Elsevier Science, Washington, D. C., 2003.
- ⁵Megson, T. H., *Aircraft Structures for Engineering Students*, Elsevier Butterworth-Heinemann, 3rd ed., 1999.
- ⁶Etkin, B. and Reid, L. D., *Dynamics of Flight, Stability and Control*, John Wiley & Sons, University of Toronto, third edition ed., 1996.
- ⁷Shields, E. J. and Testa, A. M., “Fall Migratory Flight Initiation of the Potato Leafhopper, *Empoasca fabae* (Homoptera: Cicadellia): Observations in the Lower Atmosphere Using Remote Piloted Vehicles,” *Agricultural and Forest Meteorology*, , No. 97, 1999, pp. 317–330.
- ⁸Drela, M. and Youngren, H., *Athena Vortex Lattice (AVL)*, <http://web.mit.edu/drela/Public/web/avl/>, version 3.27 ed., 2009.
- ⁹Mason, W. H., *FRICITION Manual*, Blacksburg, VA, http://www.aoe.vt.edu/~mason/Mason_f/MRsoft.html 2002-2006.
- ¹⁰John D. Anderson, J., *Aircraft Performance and Design*, McGraw Hill, New York, first edition ed., 1998.
- ¹¹Hepperle, M., *JavaProp - Design and Analysis of Propellers*, Braunschweig, Germany, 1996-2006.
- ¹²Edward A. Haering, J., “Airdata Measurement and Calibration,” NASA Technical Memorandum NASA-TM-104316, NASA DFRC, Edwards, CA, 1995.
- ¹³Bhamidipati, K. K., Uhlig, D., and Neogi, N., “Engineering Safety and Reliability into UAV Systems: Mitigating the Ground Impact Hazard,” *AIAA Guidance, Navigation, and Control Conference and Exhibit*, No. AIAA-2007-6510, AIAA, Hilton Head, SC, August 20-23 2007.
- ¹⁴Open Source, *Flightgear*, v. 1.9.1, <http://www.flightgear.org/>, 2009.